

## Features of frictional treatment of the composite NiCrBSi-Cr<sub>3</sub>C<sub>2</sub> laser clad coating

N. N. Soboleva<sup>†,1,2</sup>, A. V. Makarov<sup>3</sup>, E. P. Zavarzina<sup>3</sup>, P. A. Skorynina<sup>1</sup>, I. Yu. Malygina<sup>1</sup>

<sup>†</sup>natashasoboleva@list.ru

<sup>1</sup>Institute of Engineering Science, UB RAS, 34 Komsomolskaya St., Ekaterinburg, 620049, Russia

<sup>2</sup>Ural Federal University n. a. the first President of Russia B. N. Yeltsin, 19 Mira St., Ekaterinburg, 620002, Russia

<sup>3</sup>M. N. Miheev Institute of Metal Physics UB RAS, 18 S. Kovalevskaya St., Ekaterinburg, 620108, Russia

The authors conducted a comparative analysis of the effectiveness of frictional treatment with a sliding indenter of a NiCrBSi coating and a composite coating formed by laser cladding of a powder mixture of 85 wt.% NiCrBSi and 15 wt.% Cr<sub>3</sub>C<sub>2</sub>. The criteria were intensive strain hardening, favorable compressive stresses, and low surface roughness. Frictional treatment with an indenter made of cubic boron nitride at a load of 350 N provides less intense deformational hardening of the NiCrBSi-Cr<sub>3</sub>C<sub>2</sub> coating (microhardness growth from 900 to 940 HV 0.025) than the NiCrBSi coating (from 570 to 850 HV 0.025). This is due to the significantly higher initial hardness of the composite coating, because its structure, in addition to the phases characteristic of the NiCrBSi coating, contains large primary Cr<sub>3</sub>C<sub>2</sub> carbides, which did not dissolve during cladding, as well as elongated Cr<sub>23</sub>C<sub>6</sub> carbides, precipitated during cooling from a solid solution supersaturated with chromium as a result of the partial dissolution of Cr<sub>3</sub>C<sub>2</sub> carbides during cladding. Frictional treatment also results in a lower level of compressive residual stresses (–250 MPa) on the composite coating surface than on the NiCrBSi coating surface (–390 MPa). In contrast to frictional treatment of the NiCrBSi coating, when a smoothed surface with a nano-roughness is formed ( $R_a = 60$  nm), frictional treatment of the composite coating forms a surface with a higher roughness ( $R_a = 310$  nm) due to the creation on the surface of supporting “island frame” of large Cr<sub>3</sub>C<sub>2</sub> chromium carbides protruding 2–5 μm.

**Keywords:** laser cladding, composite NiCrBSi-Cr<sub>3</sub>C<sub>2</sub> coating, frictional treatment, microstructure, optical profilometry.

УДК: 621.791.92:621.793.09

## Особенности фрикционной обработки композиционного NiCrBSi-Cr<sub>3</sub>C<sub>2</sub> покрытия, сформированного лазерной наплавкой

Соболева Н. Н.<sup>†,1,2</sup>, Макаров А. В.<sup>3</sup>, Заварзина Е. П.<sup>3</sup>,

Скорынина П. А.<sup>1</sup>, Малыгина И. Ю.<sup>1</sup>

<sup>1</sup>Институт машиноведения УрО РАН, ул. Комсомольская, 34, Екатеринбург, 620049, Россия

<sup>2</sup>Уральский федеральный университет им. первого президента России Б. Н. Ельцина,  
ул. Мира, 19, Екатеринбург, 620002, Россия

<sup>3</sup>Институт физики металлов им. М. Н. Михеева УрО РАН, ул. С. Ковалевской, 18, Екатеринбург, 620108, Россия

Проведен сравнительный анализ эффективности фрикционной обработки скользящим индентором покрытия NiCrBSi и композиционного покрытия, сформированного газопорошковой лазерной наплавкой смеси порошков 85 масс.% NiCrBSi и 15 масс.% Cr<sub>3</sub>C<sub>2</sub>, по критериям интенсивного деформационного упрочнения, создания благоприятных сжимающих остаточных напряжений и достижения низкой шероховатости поверхности. При фрикционной обработке индентором из кубического нитрида бора при нагрузке 350 Н у покрытия NiCrBSi-Cr<sub>3</sub>C<sub>2</sub> установлено менее интенсивное деформационное упрочнение — микротвердость возросла от 900 до 940 HV 0.025, чем у покрытия NiCrBSi — от 570 до 850 HV 0.025. Это обусловлено существенно большей исходной твердостью

композиционного покрытия, в структуре которого, кроме фаз, характерных для покрытия NiCrBSi, содержатся крупные первичные карбиды  $\text{Cr}_3\text{C}_2$ , не растворившиеся при наплавке, а также вытянутые карбиды  $\text{Cr}_{23}\text{C}_6$ , выделившиеся при охлаждении из твердого раствора, пересыщенного хромом в результате частичного растворения карбидов  $\text{Cr}_3\text{C}_2$  при наплавке. Фрикционная обработка приводит также к достижению меньшего уровня сжимающих остаточных напряжений ( $-250$  МПа) на поверхности композиционного покрытия, чем на поверхности покрытия NiCrBSi ( $-390$  МПа). В отличие от фрикционной обработки NiCrBSi покрытия, когда образуется ровная выглаженная поверхность с наношероховатостью ( $R_a = 60$  нм), фрикционная обработка композиционного покрытия формирует поверхность с большей шероховатостью ( $R_a = 310$  нм) вследствие формирования на поверхности своеобразного опорного «островковкового каркаса» из выступающих на  $2-5$  мкм крупных карбидов хрома  $\text{Cr}_3\text{C}_2$ .

**Ключевые слова:** лазерная наплавка, композиционное NiCrBSi- $\text{Cr}_3\text{C}_2$  покрытие, фрикционная обработка, микроструктура, оптическая профилометрия.

## 1. Introduction

The formation of coatings with high-performance properties on the surface of machine parts and tools is an effective method for increasing their durability [1]. The deposition of NiCrBSi coatings is widely used for parts exposed to wear or corrosion [1–3].

The addition of hard particles during cladding/spraying further improves the performance of NiCrBSi coatings by creating metal-matrix composite coatings based on NiCrBSi with undissolved particles during the formation of coatings [1, 4, 5]. Additives WC/ $\text{W}_2\text{C}$ , SiC, TaC, VC, TiC can be used as strengthening carbide particles when creating composite coatings based on NiCrBSi [6–8].

Composite NiCrBSi- $\text{Cr}_3\text{C}_2$  coatings are of particular interest because they are suitable for the aviation industry due to their high wear resistance and resistance to corrosion and oxidation at high temperatures [9,10].

There are various ways to apply NiCrBSi coatings and composite coatings based on them. Laser cladding, the use of which makes it possible to obtain homogeneous layers with low mixing with the substrate, is a modern way of their formation [1,11,12].

The surface of coatings after laser cladding has a significant roughness and, as a rule, an undulated relief [13]. In the case of deposition of coatings on parts of precision friction units, when asperities and undulations of the surface are unacceptable, grinding of the clad surface with abrasive wheels is usually carried out.

In [14–16], an effective method for obtaining surface-hardened NiCrBSi coatings on metal parts is proposed. It includes gas-powder laser cladding followed by frictional treatment with a sliding hemispherical indenter made of cubic boron nitride. It is important to note that frictional treatment should be considered as a finishing technological operation, which should provide not only effective deformational hardening but also the formation of favorable compressive residual stresses in the surface layer as well as obtaining a surface with low roughness [17]. Consideration of the features of frictional treatment of composite coatings containing large particles of high-strength phases in the structure is of scientific and practical interest.

The aim of the study is to investigate the effectiveness of frictional treatment of a high-strength laser clad composite NiCrBSi- $\text{Cr}_3\text{C}_2$  coating according to the criteria of additional deformational hardening, the formation of a favorable stress state and creation of a functional surface profile.

## 2. Materials and Experimental procedure

NiCrBSi powder (chemical composition, wt.%: 0.48 C; 14.8 Cr; 2.6 Fe; 2.9 Si; 2.1 B; the rest is Ni) and a mixture of powders: 85 wt.% of NiCrBSi powder and 15 wt.% of  $\text{Cr}_3\text{C}_2$  powder was used as coating materials. The particle size of NiCrBSi powder was 40–160 microns, and  $\text{Cr}_3\text{C}_2$  powder was 50–150 microns. The substrate was a low-carbon steel plate with 0.2% C.

The radiation source for the deposition of coatings was a continuous  $\text{CO}_2$  laser with a radiation power of 1.4–1.6 kW. The cladding was performed in two passes at a speed of 160–200 mm/min, powder consumption of 2.9–3.8 g/min, the size of the laser spot on the surface of  $6 \times 2$  mm, and a shift of 4.0–4.5 mm. After cladding, the surface of the clad plates was subjected to grinding on a circular grinding machine with intensive cooling and additional polishing. After grinding and polishing, the coating thickness was 0.7–1.1 mm.

Frictional treatment was carried out on a laboratory setup in the air with a five-fold scan of the surface of NiCrBSi and NiCrBSi- $\text{Cr}_3\text{C}_2$  coatings with a hemispherical indenter made of dense cubic boron nitride DBN. The indenter moved reciprocally along the surface of the samples under a load of 350 N at an average speed of 0.013 m/s, with a stroke length of 18 mm and a transverse displacement of the indenter of 0.1 mm per double stroke. During frictional treatment, the friction force was continuously recorded. The coefficient of friction  $f$  was defined as the ratio of the friction force to the load on the indenter.

The structure and surfaces of the coatings were studied using a VEGA II XMU Tescan scanning electron microscope (SEM). To determine the roughness parameters and obtain 2-d and 3-d surface profiles, we used a Veeco WYKO NT 1100 non-contact optical profiling system, operating on the principle of an interferometric microscope [18]. Residual stresses were determined by the tilt method along the line (220) $\gamma$  using a Shimadzu XRD-7000 diffractometer. The values of the Young's modulus and Poisson's ratio for nickel (250 GPa and 0.33, respectively) were used.

Microhardness was measured using restored indentation method on a Shimadzu HMV-G21ST microhardness tester at a load of 0.245 N on a Vickers indenter. The measurement error of microhardness characteristics for 10 measurements was determined by the value of the standard deviation with a confidence level of 0.95.

### 3. Results and Discussion

Fig. 1a shows a general view of the cross-section of a sample with NiCrBSi-Cr<sub>3</sub>C<sub>2</sub> laser clad coating, which shows that large randomly located particles are present in a relatively uniform coating.

Based on the complex use of X-ray diffraction analysis and energy-dispersive X-ray microanalysis of individual structural constituents of the NiCrBSi-Cr<sub>3</sub>C<sub>2</sub> coating, its phase composition is established and shown in Fig. 1b. It can be seen that the structure contains phases characteristic of the NiCrBSi coating structure [19]: the matrix is a nickel-based  $\gamma$ -solid solution,  $\gamma$ +Ni<sub>3</sub>B eutectic, and relatively dispersed Cr<sub>23</sub>C<sub>6</sub> (A) chromium carbides. A distinctive feature of the microstructure of the NiCrBSi-Cr<sub>3</sub>C<sub>2</sub> coating is the presence of large Cr<sub>3</sub>C<sub>2</sub> carbides that did not dissolve during cladding, the melting point of which (1810°C [20]) significantly exceeds the melting point of the NiCrBSi alloy (about 1100°C). The presence in the structure of these large high-strength carbide particles with a clear interface with the surrounding matrix makes it possible to classify the NiCrBSi-Cr<sub>3</sub>C<sub>2</sub> coating as a composite coating.

Fig. 1b also shows that elongated Cr<sub>23</sub>C<sub>6</sub> (B) carbides precipitate from the chromium-supersaturated matrix near some primary Cr<sub>3</sub>C<sub>2</sub> chromium carbides partially dissolved during cladding. Cr<sub>23</sub>C<sub>6</sub> (B) carbides are larger than fine Cr<sub>23</sub>C<sub>6</sub> (A) carbides, which are the main strengthening phase of the NiCrBSi coating, which is not related to composite coatings [19]. The complete or partial decomposition of the primary Cr<sub>3</sub>C<sub>2</sub> chromium carbides during the deposition process with the formation of secondary Cr<sub>23</sub>C<sub>6</sub> or Cr<sub>7</sub>C<sub>3</sub>

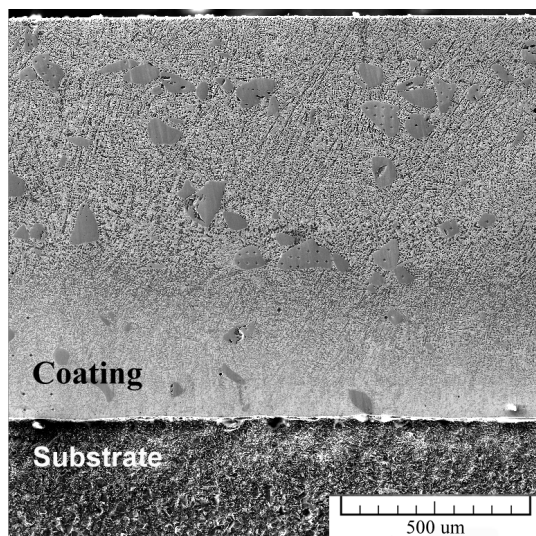
carbides is known from the literature [20,21]. Previously, using Electron Backscatter Diffraction Analysis, we showed [22] that in the studied composite NiCrBSi-Cr<sub>3</sub>C<sub>2</sub> laser clad coating, elongated large particles observed near partially dissolved primary Cr<sub>3</sub>C<sub>2</sub> carbides are chromium carbides of the Cr<sub>23</sub>C<sub>6</sub> type.

The level of the initial (before frictional treatment) hardness of the NiCrBSi coating (570 HV 0.025, Table 1) is due to the presence in its structure, along with a relatively low-strength  $\gamma$ -solid solution (with a hardness of 300–380 HV), of the  $\gamma$ +Ni<sub>3</sub>B eutectic with a hardness of 550–790 HV and the strengthening phase Cr<sub>23</sub>C<sub>6</sub> with a hardness of 1000–1150 HV [23]. Frictional treatment intensively hardens the surface of the NiCrBSi coating — up to 850 HV 0.025 (Table 1), that is, by 50%. Such intensive hardening is caused by the formation in a thin (5–7  $\mu$ m) surface layer during frictional treatment of a highly dispersed structure of a Ni-based  $\gamma$ -solid solution, which is enriched with boron, chromium, and carbon due to the deformation dissolution of nickel borides and chromium carbides, and also contains dispersed and not completely dissolved Cr<sub>23</sub>C<sub>6</sub> carbide particles [24]. The results of the works [25,26,27] also indicate the possibility of dispersion (fragmentation) and dissolution of the carbide phases under the action of frictional treatment with a sliding indenter. Along with the enhancement of the grain-boundary hardening mechanism, this leads to the activation of dispersion and solid-solution hardening mechanisms.

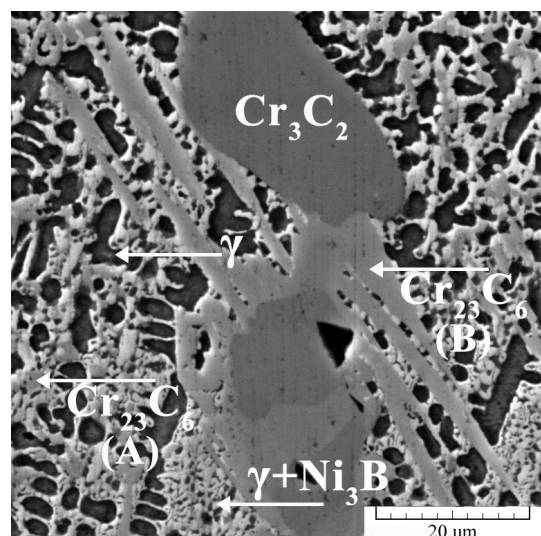
Table 1 also shows that in the polished state, the composite NiCrBSi-Cr<sub>3</sub>C<sub>2</sub> coating is characterized by an even higher hardness (900 HV 0.025). This is due to the

**Table 1.** Microhardness HV 0.025, residual stress RS and arithmetic average roughness  $R_a$  roughness of the area  $43 \times 56 \mu\text{m}$  for the laser clad coatings after different treatments.

Coating	Treatment	HV 0.025	RS, MPa	$R_a$ , nm
NiCrBSi	Polishing	570 ± 10	-120	255
	Frictional treatment	850 ± 20	-390	60
NiCrBSi-Cr <sub>3</sub> C <sub>2</sub>	Polishing	900 ± 100	-70	275
	Frictional treatment	940 ± 70	-250	310



a



b

**Fig. 1.** Cross-sectional view (a) and microstructure (b) of the NiCrBSi-Cr<sub>3</sub>C<sub>2</sub> laser clad coating (SEM).

presence in the coating structure of the high-strength  $\text{Cr}_3\text{C}_2$  phase, the hardness of which, according to the measurement results, reaches 2220 HV 0.1, as well as an additional amount of large elongated  $\text{Cr}_{23}\text{C}_6$  carbides (see Fig. 1b). As a result of frictional treatment, the microhardness on the surface of the NiCrBSi- $\text{Cr}_3\text{C}_2$  coating increases to 940 HV 0.025. Consequently, frictional treatment leads only to a slight (about 5%) deformational hardening of the composite coating, whose structure contains a large quantity of high-strength carbides, which are not hardened by frictional treatment.

According to Table 1, frictional treatment generates a lower level of favorable (contributing to increasing the durability of products) compressive residual stresses ( $-250$  MPa) in the surface layer of the NiCrBSi- $\text{Cr}_3\text{C}_2$  coating than on the surface of the NiCrBSi coating ( $-390$  MPa). This may be due to the greater deformation during frictional treatment of the NiCrBSi coating containing a larger proportion of the metal base than the composite NiCrBSi- $\text{Cr}_3\text{C}_2$  coating containing hard-to-deform large primary chromium carbides in the structure.

Table 1 also shows that the surface roughness of the NiCrBSi coating as a result of frictional treatment decreases to the level of nano-roughness ( $R_a=60$  nm). However, the surface of the composite NiCrBSi- $\text{Cr}_3\text{C}_2$  coating after frictional treatment has significantly (5 times) higher values of the roughness parameter ( $R_a=310$  nm).

Studies of surfaces after frictional treatment using scanning electron microscopy show that the NiCrBSi coating, which does not contain large strengthening phases in the structure, is characterized by a uniformly smoothed surface (Fig. 2a), while the surface of the NiCrBSi- $\text{Cr}_3\text{C}_2$  coating has non-uniform (discontinuous) areas of a rounded shape (Fig. 2b). According to the elemental mapping data (Fig. 2c), these areas contain an increased concentration of chromium and, consequently, are large  $\text{Cr}_3\text{C}_2$  chromium carbides, which are present in the structure of the composite coating (Fig. 1b) and have significantly higher hardness compared to the hardness of elongated  $\text{Cr}_{23}\text{C}_6$  chromium carbides.

The profilometry results show (Fig. 3a,b) that after frictional treatment according to the used technological modes, large hard-to-deform  $\text{Cr}_3\text{C}_2$  chromium carbides

remain on the surface of the NiCrBSi- $\text{Cr}_3\text{C}_2$  coating, protruding above the smoothed surface. This is due to the predominant deformation of the less strong and more plastic coating matrix. A similar effect of the formation of a protruding wear-resistant frame of solid particles of strengthening phases on the abrasive wear surface of a Ni-based laser clad coating was observed in [23]. The analysis shows that  $\text{Cr}_3\text{C}_2$  particles protrude above the smoothed surface of the composite coating to a height of  $2-5$   $\mu\text{m}$  (see Fig. 3c), forming a profile with a supporting "island frame" of high-strength particles (see Fig. 3a). The observed slight undulation (with a step of  $0.1$  mm) of the coating surface in the area that does not contain large chromium carbides is associated with a transverse displacement of the indenter by  $0.1$  mm for each double longitudinal stroke during frictional treatment (Fig. 3d).

#### 4. Conclusion

In contrast to the NiCrBSi laser clad coating, which as a result of frictional treatment with a sliding indenter made of cubic boron nitride in air at a load of  $350$  N is intensively hardened (microhardness increases from  $570$  to  $850$  HV 0.025, i.e. by 50%), the composite NiCrBSi- $\text{Cr}_3\text{C}_2$  coating is characterized by only a slight (up to 5%) hardening during frictional treatment in a similar mode. The established low ability to deformational hardening of the NiCrBSi- $\text{Cr}_3\text{C}_2$  coating is a consequence of the extremely high initial level of its hardness ( $900$  HV 0.025). This is due to the presence in the structure of hard (hardness up to  $2220$  HV 0.1) primary  $\text{Cr}_3\text{C}_2$  chromium carbides and large elongated secondary  $\text{Cr}_{23}\text{C}_6$  chromium carbides, precipitated near some partially dissolved  $\text{Cr}_3\text{C}_2$  carbides during cooling from a solid solution supersaturated with chromium in the process of cladding.

Frictional treatment forms favorable compressive residual stresses in the surface layer of the composite coating. However, a lower stress level ( $-250$  MPa) is achieved than in the case of the frictional treated NiCrBSi coating ( $-390$  MPa).

An important distinctive feature of the frictional treatment of the composite NiCrBSi- $\text{Cr}_3\text{C}_2$  coating is obtaining a smoothed surface with  $\text{Cr}_3\text{C}_2$  chromium carbides protruding  $2-5$   $\mu\text{m}$ . The formation on the surface of the composite

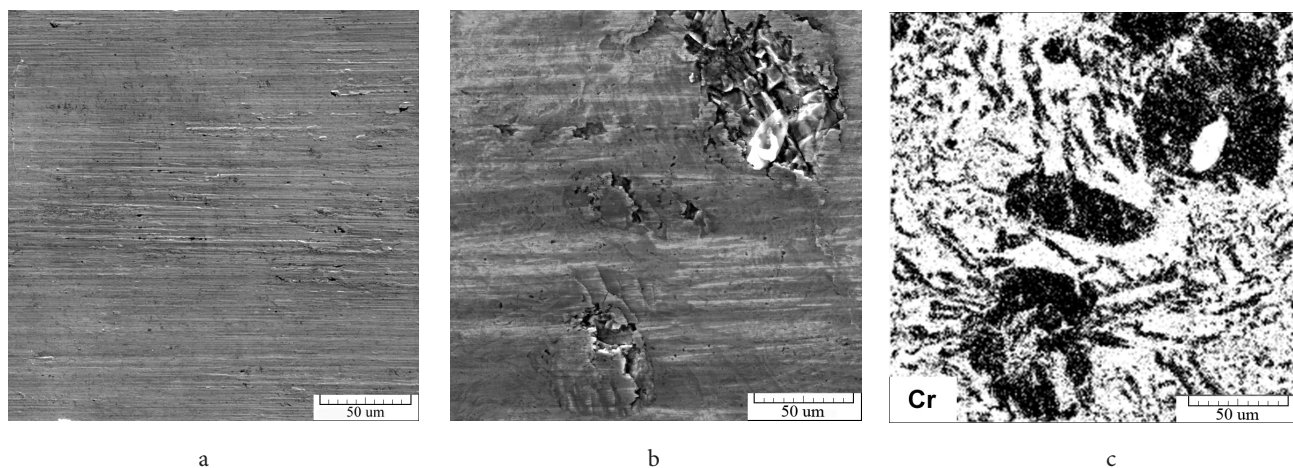


**Fig. 2.** Surfaces of the NiCrBSi (a) and NiCrBSi- $\text{Cr}_3\text{C}_2$  (b) laser clad coatings after frictional treatment and the chromium distribution at the "b" area (c) (SEM).

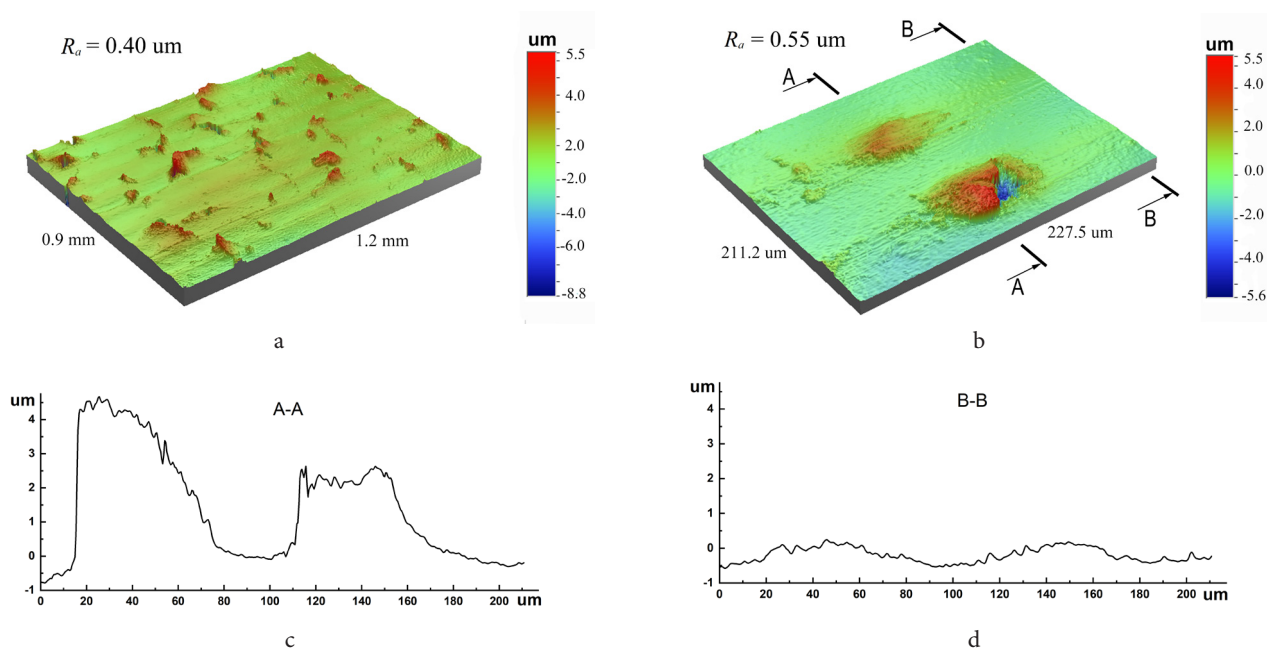


**Fig. 3.** (Color online) 3-d (a, b) and 2-d (c, d) surface profiles of the NiCrBSi-Cr<sub>3</sub>C<sub>2</sub> laser clad coatings after frictional treatment.

coating of such a profile with a specific supporting “island frame” of protruding high-strength particles is accompanied by a significantly higher roughness ( $R_a = 310$  nm) compared to the nano-roughness ( $R_a = 60$  nm), which is characterized by the surface of the NiCrBSi coating, uniformly smoothed by frictional treatment.

*Acknowledgments.* The work was performed with the financial support of the Grant from the President of the Russian Federation for young scientists MK-391.2019.8 and at the expense of funds making up the income from the trust management of the target capital for the development of UrFU, formed with the participation of UMMC-Holding Corp, as well as within the state order for IES UB RAS (AAAA-A18-118020790147-4) and IMP UB RAS (AAAA-A18-118020190116-6 and AAAA-A19-119070490049-8). The experimental research was performed on the equipment of the Plastometriya Collective Use Center of IES UB RAS.

## References

- L. E. Afanasieva, G. V. Ratkevich. Letters on Materials. 8 (3), 268 (2018). (in Russian) [Л. Е. Афанасьева, Г. В. Раткевич. Письма о материалах. 8 (3), 268 (2018).] [Crossref](#)
- B. Cai, Y.-f. Tan, L. He, H. Tan, L. Gao. Trans. Nonferrous Met. Soc. China. 23 (6), 1681 (2013). [Crossref](#)
- R. A. Savrai. Phys. Metals Metallogr. 119 (10), 1070 (2018). [Crossref](#)
- J. Yang, F. Liu, X. Miao, F. Yang. J. Mater. Process. Technol. 212 (9), 1862 (2012). [Crossref](#)
- A. V. Makarov, N. N. Soboleva, I. Yu. Malygina, A. L. Osintseva. Diagnostics, Resource and Mechanics of materials and structures. 3, 83 (2015). (in Russian) [А. В. Макаров, Н. Н. Соболева, И. Ю. Малыгина, А. Л. Осинцева. Diagnostics, Resource and Mechanics of materials and structures. 3, 83 (2015).] [Crossref](#)
- Q. Li, G. M. Song, Y. Z. Zhang, T. C. Lei, W. Z. Chen. Wear. 254 (3-4), 222 (2003). [Crossref](#)
- M.-j. Chao, W.-l. Wang, E.-j. Liang, D. Ouyang. Surf. Coat. Technol. 202 (10), 1918 (2012). [Crossref](#)
- A. V. Makarov, Yu. S. Korobov, N. N. Soboleva, Yu. V. Khudorozhkova, A. A. Vopneruk, P. Balu, M. M. Barbosa, I. Yu. Malygina, S. V. Burov, A. K. Stepchenkov. Letters on Materials. 9 (4), 470 (2019). [Crossref](#)
- A. Zikin, I. Hussainova, C. Katsich, E. Badisch, C. Tomastik. Surf. Coat. Technol. 206 (19-20), 4270 (2012). [Crossref](#)
- A. C. Karaoglanli, M. Oge, K. M. Doleker, M. Hotamis. Surf. Coat. Technol. 318, 299 (2017). [Crossref](#)
- A. S. C. M. d'Oliveira, R. Vilar, C. G. Feder. Appl. Surf. Sci. 201 (1-4), 154 (2002). [Crossref](#)
- A. N. Cherepanov, A. M. Orishich, V. E. Ovcharenko, A. G. Malikov, V. O. Drozdov, A. P. Pshenichnikov. Phys. Metals Metallogr. 120 (1), 101 (2019). [Crossref](#)
- R. Singh, D. Kumar, S. K. Mishra, S. K. Tiwari. Surf. Coat. Technol. 251, 87 (2014). [Crossref](#)
- N. N. Soboleva, A. V. Makarov, I. Yu. Malygina. Obrabotka Metallov — Metal Working and Material Science. 61 (4), 79 (2013). (in Russian) [Н. Н. Соболева, А. В. Макаров, И. Ю. Малыгина. Обработка металлов. Технология, оборудование, инструменты. 61 (4), 79 (2013).]
- N. N. Soboleva, A. V. Makarov, I. Yu. Malygina, R. A. Savrai. AIP Conf. Proc. 1785, 030028 (2016). [Crossref](#)
- Патент РФ № 2709550, 18.12.2019. (in Russian) [Патент РФ № 2709550, 18.12.2019.]
- A. V. Makarov, L. G. Korshunov. Phys. Metals Metallogr. 120 (3), 303 (2019). [Crossref](#)
- S. V. Smirnov, D. A. Konovalov, S. T. Kalashnikov, E. O. Smirnova. Diagnostics, Resource and Mechanics of materials and structures. 5, 106 (2018). (in Russian) [С. В. Смирнов, Д. А. Коновалов, С. Т. Калашников,

- E. O. Смирнова. Diagnostics, Resource and Mechanics of materials and structures. 5, 106 (2018).] [Crossref](#)
19. R. A. Savrai, A. V. Makarov, N. N. Soboleva, I. Yu. Malygina, A. L. Osintseva. J. Mater. Eng. Perform. 25 (3), 1068 (2016). [Crossref](#)
  20. X. Ping, S. Sun, F. Wang, H. Fu, J. Lin, Y. Lin, Y. Lei. Surf. Rev. Lett. 26 (6), 1850207 (2018). [Crossref](#)
  21. Š. Houdková, J. Černý, Z. Pala, P. Haušild. Key Eng. Mater. 662, 111 (2015). [Crossref](#)
  22. R. A. Savrai, A. V. Makarov, E. S. Gorkunov, N. N. Soboleva, L. Kh. Kogan, I. Yu. Malygina, A. L. Osintseva, N. A. Davydova. AIP Conf. Proc. 1915, 040049 (2017). [Crossref](#)
  23. A. V. Makarov, N. N. Soboleva, I. Yu. Malygina. J. Frict. Wear. 38 (4), 272 (2017). [Crossref](#)
  24. A. V. Makarov, N. N. Soboleva, R. A. Savrai, I. Yu. Malygina. Vektor nauki Tolyattinskogo gosudarstvennogo universiteta. 34 (4), 60 (2015). (in Russian) [A. В. Макаров, Н. Н. Соболева, Р. А. Саврай, И. Ю. Мальгина. Вектор науки Тольяттинского государственного университета. 34 (4), 60 (2015).] [Crossref](#)
  25. A. V. Makarov, R. A. Savrai, N. A. Pozdejeva, S. V. Smirnov, D. I. Vichuzhanin, L. G. Korshunov, I. Yu. Malygina. Surf. Coat. Technol. 205 (3), 84 (2010). [Crossref](#)
  26. R. A. Savrai, A. V. Makarov, I. Yu. Malygina, E. G. Volkova. Mater. Sci. Eng., A. 734, 506 (2018). [Crossref](#)
  27. A. V. Makarov, R. A. Savrai, P. A. Skorynina, E. G. Volkova. Met. Sci. Heat Treat. 62 (1-2), 61 (2020). [Crossref](#)